

Research Article

# Synthesis and Characterization of Nanostructure $TiO_2$ /Anthraquinone (AQ) Prepared by Sol-Gel Method

Ramzei R. Al-Ani, Yousif K. Abdul Amir, Fadhela M. Hussein

Department of Chemistry, College of Science, Mustansiriyah University, IRAQ.

\*Correspondent email: fadhusein\_99@yahoo.com

## Article Info

Received  
26/6/2016

Accepted  
14/11/2016

## Abstract

Sol-gel technique conducted to synthesize nano titanium dioxide with anthraquinone (AQ) relatively in acidic pH. Nanoparticles were characterized using techniques like, Scanning Electron Microscope (SEM), Atomic Force Microscope (AFM), UV-Visible Spectroscopy, X-ray diffraction (XRD), Fourier transform infrared (FT-IR), SEM picture display that the  $TiO_2$ /AQ is spherical in style, the band gap of  $TiO_2$ /AQ nanoparticle is (3.05eV), BET and BJH analysis provides Pore volume and specific Surface area and the kinetic studie Suggest that the reaction is pseudo first order and the rate of reaction was reduce with rising initial concentration for p-Nitrotolune.

**Keywords:** sol-gel, Nanoparticles, Atomic Force Microscope, Nanostructure.

## الخلاصة

تم خلال البحث الحالي دراسة تحضير الدقائق النانوية لثنائي اوكسيد التيتانيوم مع انثراكوينون بطريقة الهلام-جل) واستخدمت التقنيات الاشعة السينية ومجهر الماسح الالكتروني ومجهر القوة الذرية ومطياف الاشعة فوق البنفسجية والاشعة تحت الحمراء و تم دراسة خصائص وتشخيص المادة النانوية المحضرة ووجد ان الدقائق النانوية كروية الشكل ذات حجوم مختلفة ان فجوة الطاقة للمادة النانوية لايجاد المساحة السطحية وحجم المسام. *BET, BJH* وقد استخدم تحليل  $3.05 eV$  كما درس تأثير الكفاءة الضوئية لتجزئة بارا نايتروتولوين في المحاليل المائية وكان التفاعل من المرتبة الاولى الكاذبة وسرعة التفاعل تنخفض بزيادة التركيز الابتدائي.

## Introduction

In the other few years, major efforts have been synthetic to convert the band structure of  $TiO_2$  to shift its absorption border across the visible light region and site its band borders at proper placement, thus clement, its photocatalytic efficiency one way of doing thus is to dope  $TiO_2$  with each anions or cations [1].

Titanium dioxide have three crystal kind rutile, anatase, and brookite of these various, anatase  $TiO_2$  has been most excessively use as a widespread catalyst in order that of its diverse fitness, like as visual and electronic ownership, crest photo-catalytic efficiency, least cost, nontoxicity and while chemical stabilization. The catalytic activity of  $TiO_2$  is likely on its dependent on the crystal size the minimal the particles, the great will be its surface area [2].

The sol-gel method is the extreme succeeded for providing nanosized metal oxide semiconductor, sol-gel derived  $TiO_2$  powder has been report to show height, catalytic efficiency due to their end texture broad surface and height porosity [3] [4].

The sol-gel method is a depressed temperature way extreme hard used to acquire best ceramic [5]. Several methods used to improve the stability of nanoparticles, like torpidity of semiconductor and cap by kind organic or inorganic category.

Through these methods, polymer cap in a chemical way advanced to synthesize nanoparticles with high surface stability, and also have significant effect on the morphology and optic property of nanoparticle, doping of  $TiO_2$  have been an important access in energy gap engineering to charge the optic repayment of semiconductor photo catalyst [6].

More way has been based for titanium dioxide synthesis like sol-gel method, hydrothermal technique, chemical steam deposition, direct oxidation and all the other.

The sol-gel method is one of the extreme used techniques led to its chance of deriving single metasTable frame at depressed reaction temperatures and stellar chemical homogeneity [7].



## Material and Methodologies

Whole reagents used were of analytical stage purity and was obtained from Merck chemical Reagent Co. LTD. titanium tetra isopropoxide (TTIP) and anthraquinone (Sigma, Aldrich), ethanol absolute (Merck) while deionization water consumed for the concoction of nanoparticle by the sol-gel method.

## Characterization

The prepared crystalline nanoparticles structure was characterized using Surface morphology by using SEM (Sigma). UV-visible absorption spectrum of nanocrystal was recorded in the wave length range (200-800nm) using two quartz cells of (10mm) path way with double beam spectrophotometer (100 Conc/Varian. USA) and the mean, particle space was measured employing atomic force microscope (AFM) AA300 scanning probe microscope angstrom Advanced Inc. The surface area of nanoparticle was calculated by employing Instrument NOVA station A by nitrogen

## Nano Particles Preparation

(a) Assembly of titanium dioxide was acquired from titanium tetra isopropoxide (TTIP) which were settled in absolute ethanol and deionization water the admixture were designed in expression of a molar ratio of TTIP: H<sub>2</sub>O = 1: 4 Nitric acid was consumed to detect pH=4 and for hold the hydrolysis operation of the solution. The sol was busily whiskered for 60 min in require to brew a homogenous sol. After 24 hour the sol was convert into gel to acquire nanoparticle, the gel was dried under 80<sup>0</sup>C till 2 hours to vaporize water and organic material to the upper range, then the dry gel was calcination at different temperatures for 2 hours were subsequently carried outside to acquire coveted titanium dioxide nanoparticles [7] [8]

(b) Anthraquinone/TiO<sub>2</sub> was prepared by capped technique (TiO<sub>2</sub> with Anthraquinone) by Sol-Gel. (0.2 gm) anthraquinone was dissolved in absolute ethanol and hydrolyze through addition of step (A) solution down fixed stirring at room temperature for 40 minute then cooled at room temperature, separated by centrifuge for 15 min, the absolute ethanol and water with washed and the resultant material was aging for 24 hour and dried at 80<sup>0</sup>C for 4 hours.

## Results and Discussion

The study surface roughness and characteristics of AQ doped TiO<sub>2</sub> nanoparticles Surface morphology photographs was recorded by using SEM, AFM, surface area and XRD.

**X-rays** the crystal texture of the acquired powder was describe by powder X-ray diffraction (XRD) analyses. As it is indicate in Figure 1, the diffraction peaks that indexed as the anatase phase for titanium dioxide accord to the JCPDS card No., 21-1276.

The main diffraction peaks at 2θ=25.34, 37.80, 48.07, 53.80 and 55.07<sup>0</sup> are belong to (101), (004), (200), (105) and (211) planes of the TiO<sub>2</sub> tetragonal phase, Figure 1 shows a powerful peak agree at 2θ = 25.34<sup>0</sup> which correspond to the (101) reflection, while another characteristic peak (004), (200), (105) and (211) correspond to various crystalline planes. In the status of the sample acquired with the use of the AQ, the XRD patterns display weakened peak occurring at 2θ =23.5, 27.4, 62.7, 68.9, 70, and 75.12<sup>0</sup> corresponds to the AQ structure. The analyses of the datum due to the conclusion that the increment of AQ at the stage of titanium dioxide syntheses, titanium dioxide sample with the addition of AQ caused worthy changes in crystals characteristic. It mean sample designed with the tiny addition of AQ are characterized with the large crystallite sizes was (24.19 nm) calculated using Scherrer formula.

$$D = K \lambda / B \cos \theta \quad (1)$$

Where D is the crustallite volume, λ is wavelength of the X-ray wherever D is the crustallite volume, radiation (Cu K α = 0.15418 nm), K is the Scherrer constant and B is the fall widths at half maximums height, θ is the Bragg diffraction angles. Our observations are in agreement with Stefanska *et al.* [9] studies effect of increment of acetyl acetone as chelating factor on the property.

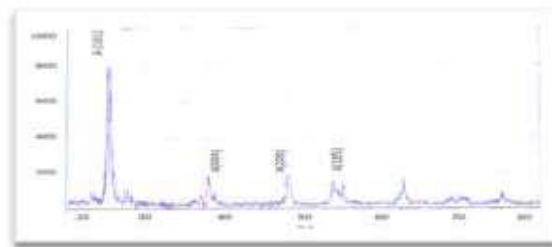


Figure 1: X-ray diffraction (XRD) of TiO<sub>2</sub>/AQ nanoparticle.

**SEM** morphologies of the Nano crystalline AQ doped  $\text{TiO}_2$  is depicted in Figure 2 shows SEM image of the prepared nanoparticle obtained by sol-gel method was showed spherical structure. The average diameter of  $\text{TiO}_2$ /AQ nanoparticle is clear nanostructure can be seen having (65 nm). The nanoparticle seen by SEM picture depends of a number of crystallite that is seen by TEM picture 200 nm.

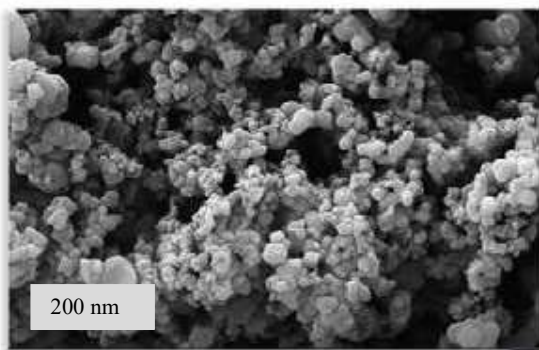


Figure 2: SEM image of  $\text{TiO}_2$  /AQ nanoparticle

**AFM** imaging Figure 3 display that the average diameter of the particle were (73.34 nm) that diameter was huge than the value acquired from SEM picture analyses (65 nm). The Root Mean Square lead to be 2.33 nm on the plain  $\text{TiO}_2$ /AQ surface. It is fully known that AFM gives stellar resolution for higher resolution imaging [10].

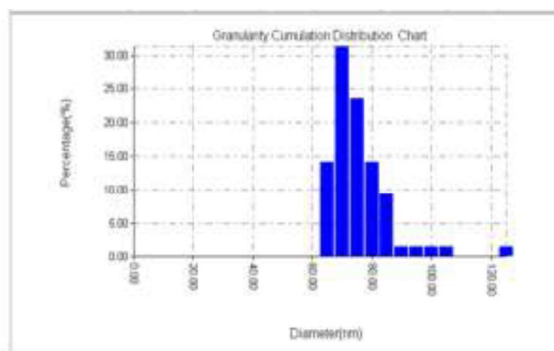
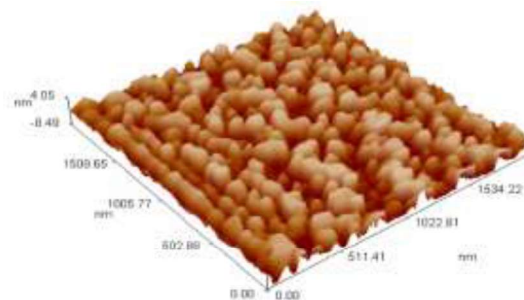


Figure 3: AFM 2, 3D topography map of  $\text{TiO}_2$ /AQ nanoparticle.

**TEM** pictures of sol-gel derive nanoparticle is show in Figure 4 express spherical structure can be seen that have a diameter of (30 nm). The particle size measure through TEM was ordinarily in approval with those determined by XRD although some agglomeration current, led to tip surface energy of the particle. Stefanska *et al.* [9] studied  $\text{TiO}_2$  particles prepared with acetylaceton as chelating factor addition display spherical particle and tight size division.

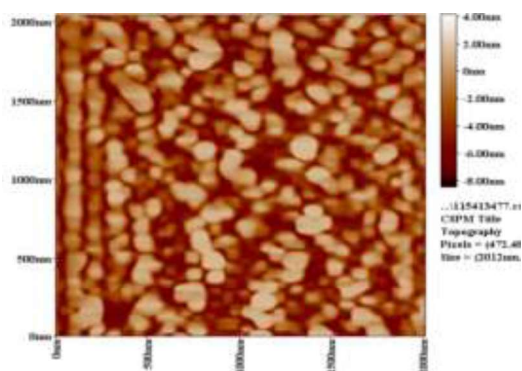


Figure 4: TEM image of  $\text{TiO}_2$ /AQ nanoparticle.

**FTIR** spectra of nanoparticles of anthraquinone and  $\text{TiO}_2$  were recorded to study the functional group and binding sites.

FTIR spectra of AQ is shown in Figure 5, the assignments of absorption band in the spectra as the band located at 1672.3 cm<sup>-1</sup> and 690 cm<sup>-1</sup> are led to the stretching and bending vibration of the C=C bond. The band at 1631.83 cm<sup>-1</sup> in spectra was led to the bending vibration of the C=O bond. It can be seen in the band at 1573.97 cm<sup>-1</sup> indicating a presence of C-C bond and 1330 cm<sup>-1</sup> was led to C-H bond.

The FTIR spectrum of TiO<sub>2</sub>/AQ is shown in Figure 6 a band was appeared at 633, 603 cm<sup>-1</sup> was referred to Ti-O bending mode.

The band at 1450.22 cm<sup>-1</sup> agrees to the Ti-O-Ti bonding. While the bands at 1672, 1573, 1330, 1168, and 690 cm<sup>-1</sup> has been reduced after nanoparticle TiO<sub>2</sub>/AQ formation. The band at 2350 cm<sup>-1</sup> was due to C=O stretching vibration and a very small bend appeared at 1406.15 cm<sup>-1</sup>.



Figure 5: FTIR spectrum of AQ.

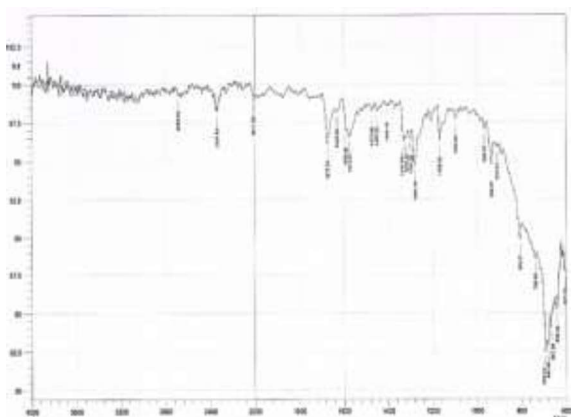


Figure 6: FTIR spectra of TiO<sub>2</sub>/AQ nanoparticle.

### Determination of Band Gap of TiO<sub>2</sub>/AQ Nanoparticle

The band of bulk anatase is 3.2 eV after doping by AQ a tiny change were spotted led to the

existence of anatase nanocrystallite the absorbance that seem at energies below the band gap energy while AQ were present in content results in higher insparency in the visible region which leads to higher dispersity, and smaller particle size [11]. The band gap was determined by using Tauc Equation [12] is described accordingly:

$$(\alpha h\nu)^{1/n} = A (h\nu - E_g) \quad (2)$$

Where A is a constant,  $\alpha$  is absorption coefficient, and  $E_g$  is the energy gap of material and exponent (n) consist on the kind of transition. To determine the likely transition  $(\alpha h\nu)^{1/n}$  vs  $h\nu$  is plot and congruent band gap was acquired from extrapolate the part of the graph on  $h\nu$  axis as the energy gap value of TiO<sub>2</sub>/AQ is found to be (3.05 eV).

### Surface Area and Porosity of TiO<sub>2</sub> /AQ Nanoparticles

BET and BJH methods were conducted for determination of surface area analysis and porosity analysis. That AQ doped TiO<sub>2</sub> resulted in break down of the mesoporous surface area decrease to 15.96 m<sup>2</sup>.g<sup>-1</sup>. The situation of that band is influenced by the coordinate geometry round the titanium atom and by the existence of adsorbent as shown in Table 1, Table 2, and Figure 7. Note that TiO<sub>2</sub> in the case of doping with AQ less surface area while increase average pore diameter from 104.2 Å to 365.5 Å.

Komarneni *et al.* [13] determined the surface area of anatase and doped polyvinylpyrrolidone (PVP) during microwave-hydrothermal method which was equal (77 m<sup>2</sup>.g<sup>-1</sup>) because the presence of PVP did not disperse anatase.

Table 1: Surface area and pore size of TiO<sub>2</sub>/AQ

Pore vol. cm <sup>3</sup> .g <sup>-1</sup>	Pore diam. Å	Avg. pore diam. Å	Surface area m <sup>2</sup> .g <sup>-1</sup>	Sample
0.3528	87.70	104.2	129.8	TiO <sub>2</sub>
0.1498	30.79	365.5	15.96	AQ/TiO <sub>2</sub>

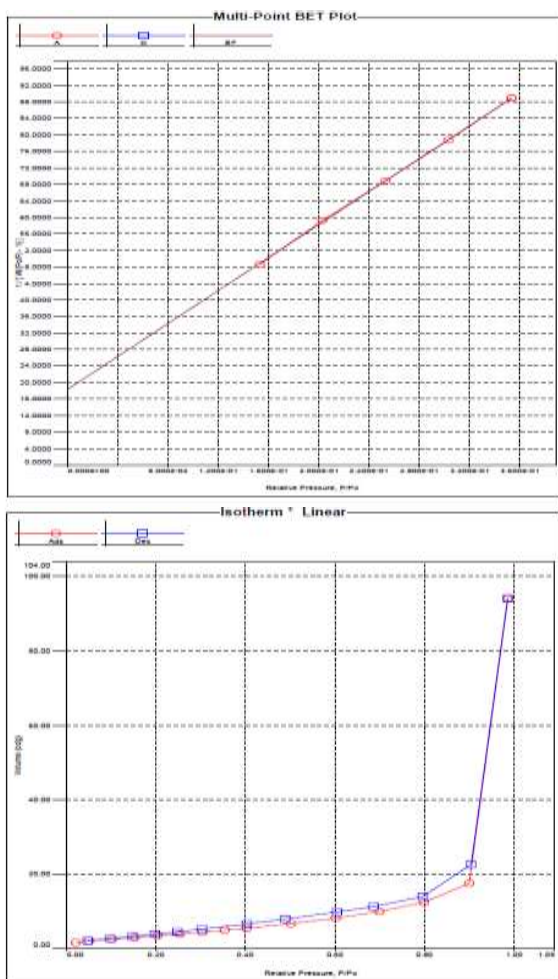


Figure 7: Surface area of TiO<sub>2</sub>/AQ.

Table 2: Surface area and pore volume of TiO<sub>2</sub>/AQ

Multi-Point BET					
Relative Pressure [P/P <sub>0</sub> ]	Volume@STP [cc/g]	1/[W((P <sub>0</sub> P) - 1)]	Relative Pressure [P/P <sub>0</sub> ]	Volume@STP [cc/g]	1/[W((P <sub>0</sub> P) - 1)]
1.52943e-01	2.9720	4.8609e+01	3.03383e-01	4.2234	7.8776e+01
2.03048e-01	3.4371	5.9310e+01	3.53333e-01	4.9148	8.8951e+01
2.52884e-01	3.9309	6.8895e+01			

MBET summary			
Slope =	199.855		
Intercept =	1.832e+01		
Correlation coefficient, r =	0.999862		
C constant =	11.908		
Surface Area =	15.962 m <sup>2</sup> /g		

Single Point Surface Area				
Relative Pressure [P/P <sub>0</sub> ]	Volume@STP [cc/g]	1/[W((P <sub>0</sub> P) - 1)]	Slope	Surf. Area [m <sup>2</sup> /g]
3.53333e-01	4.9148	8.8951e+01	261.7489	13.8533

BJH Pore Size Distribution Description							
Diameter [nm]	Pore Volume [cc/g]	Pore Surf. Area [m <sup>2</sup> /g]	dV(d) [cc/nm]	dS(d) [m <sup>2</sup> /nm]	dV(logd) [cc/g]	dS(logd) [m <sup>2</sup> /g]	
1.4139	2.0002e+00	0.0000e+00	0.0000e+00	0.0000e+00	0.0000e+00	0.0000e+00	0.0000e+00
1.6500	5.8715e-04	1.2075e-03	0.0000e+00	4.8338e+00	7.8351e-03	1.8665e-01	1.8665e-01
1.9279	1.2110e-03	2.6679e-03	2.8626e-03	5.9395e+00	1.2650e-02	2.8330e-01	2.8330e-01
2.1901	2.1719e-03	4.4304e-03	3.7141e-03	6.8149e+00	1.8623e-02	3.4158e-01	3.4158e-01
2.4520	3.1835e-03	6.0744e-03	3.3154e-03	5.3891e+00	1.6775e-02	3.0506e-01	3.0506e-01
2.9200	5.5295e-03	9.2749e-03	3.6947e-03	5.2409e+00	2.4846e-02	3.3896e-01	3.3896e-01
3.5969	8.3814e-03	1.2336e-01	1.9924e-03	4.4956e+00	3.2715e-02	3.9382e-01	3.9382e-01
4.6109	1.1312e-02	1.4964e-01	2.3950e-03	1.9550e+00	2.3699e-02	2.0724e-01	2.0724e-01
6.0178	1.3384e-02	1.6340e-01	1.4263e-03	9.3472e-01	1.9389e-02	1.2887e-01	1.2887e-01
8.0280	1.7405e-02	1.8210e-01	1.0850e-03	5.0417e-01	2.1169e-02	9.3366e-02	9.3366e-02
16.0167	3.2737e-02	2.2035e-01	1.3920e-03	3.4454e-01	4.6783e-02	1.2183e-01	1.2183e-01
81.5266	1.5193e-01	2.7947e-01	9.8737e-04	4.8459e-02	1.4483e-01	7.1121e-02	7.1121e-02

BJH desorption summary		
Surface Area =	27.847 m <sup>2</sup> /g	
Pore Volume =	0.161 cc/g	
Pore Diameter Dv(d) =	3.597 nm	

## Kinetic Study

### Influence of Concentration of Nanoparticle TiO<sub>2</sub>/AQ

The removal efficiency of concentration of TiO<sub>2</sub>/AQ on para-nitrotoluene photodegradation is illustrated in Figure 8.

It indicates the decay of p-N.T increased with loading of catalyst up to (0.075 g/l) and 96 % degradation efficiency. The optimum of catalyst load TiO<sub>2</sub>/AQ nanoparticle was calculated during the scope of 0.025 g/l to 0.25 g/l at pH 5.7 and initial concentration of p-N.T (1\*10<sup>-4</sup> M). The efficiency of p-N.T photodegradation is reduced at higher concentration of catalyst (0.25g/l). The explanation of this phenomenon is that light intensity will be decreased by the suspension of catalyst at high concentration and radical generated is decrease [14].

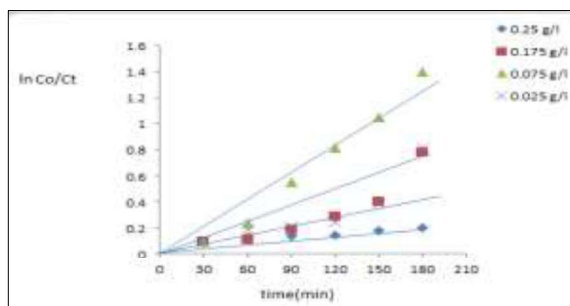


Figure 8: Different loading of nanoparticle TiO<sub>2</sub>/AQ, P-N.T (1x10<sup>-4</sup>).

### Effect of Initial Concentration of P-Nitrotoluene

Photodecomposition reaction seemed to obey a pseudo first – order reaction kinetics, as the results obtained fitted this reaction Equation. The influence is of changing p-NT concentration at scope (1-7 x10<sup>-4</sup>M).

The rate constant of the photoreactions were (0.0103 min<sup>-1</sup>) in the presence of catalysis at pH

5.7 The degradation efficiency of p-N.T was as maximum value at  $1 \times 10^{-4}$  M where as concentration more than  $1 \times 10^{-4}$  M degradation efficiency decreased within 180 min at same conditions of experiment as shown in Figure 9. More molecules covering the surface of TiO<sub>2</sub> /AQ reduce of photon absorption. This result has effects on hydroxyl radicals generation which decreases the efficiency degradation

At substrate concentrations, yet the photonic activity reduce and TiO<sub>2</sub> /AQ surface turn into saturated main to catalyst extinction [15].

1/rate was plotted versus 1/Co based on the data as shown in Figure 10 1/rate correlated to 1/Co well, so the degradation of 4-N.T catalyzed TiO<sub>2</sub>/AQ fitted with the Langmuir Hinshelwood (L-H) kinetic model according to Equation 1.

$$1/r = 1/k + 1/kKCo \quad (3)$$

Where k and K are estimated ( $416.67 \times 10^{-7} \text{ M}^{-1} \text{ min}^{-1}$ ) and ( $266.397 \text{ M}^{-1}$ ) respectively. The high value of adsorption constant (K) indicates to a stronger adsorption on sites at TiO<sub>2</sub> surface.

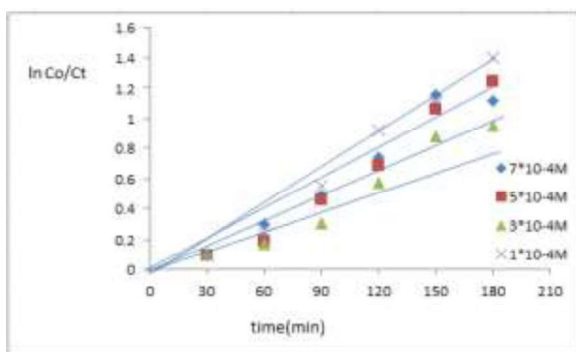


Figure 9: Different concentration of p-N.T, TiO<sub>2</sub>/AQ nanoparticle (0.075 g/l), pH 5.7.

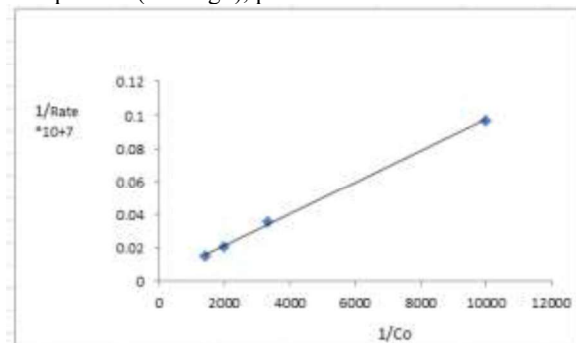


Figure 10: plot of the reverse of the initial rate of p-N.T in TiO<sub>2</sub>/AQ nanoparticle (0.075g/l) against the reverse of the initial p-N.T concentration.

### Effect of PH Value (TiO<sub>2</sub>/AQ)

The photocatalytic treatment of p-N.T in the presence of the nanoparticle (TiO<sub>2</sub>/AQ) proved to be quite effective one the degradation and mineralization of the toxicity. The rate of photocatalytic degradation was studied in the pH range (3-9) by UV-light, TiO<sub>2</sub>/AQ loading 0.075 g/l and initial concentration of p-N.T ( $1 \times 10^{-4}$  M). The maximum degradation was obtained at pH value 5.7 as shown in Figure 11. As pH raise, this will increase the degeneration activity over to pH 5.7, the extreme 96% degeneration activity were acquired at pH 5.7 can be explain by surface charges on the various photocatalyst.

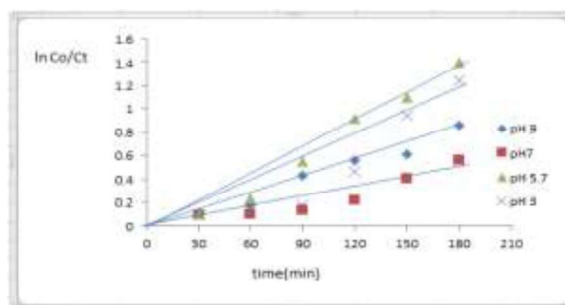


Figure 11: Different pH of TiO<sub>2</sub> /AQ (0.075g/l), p-N.T ( $1 \times 10^{-4}$  M)

### Effect of Temperature on Photo degradation of P-N.T by TiO<sub>2</sub>/AQ Nanoparticle.

The rate constant was evaluated at each temperature their results are shown in Figure 12. The photocatalytic degradation reaction for p-NT has been load out by convert the reaction temperature from 288k to 318 k The temperature effect of photodegradation of 4-N.T at initial concentration ( $1 \times 10^{-4}$  M), pH 5.7, and (0.075 g/l) of TiO<sub>2</sub> /AQ at 298 K a higher degradation efficiency 96 %. There are in approval with the Arrhenius Equation for that the rate constant ln k must rise linear for reciprocal temperature. Arrhenius land of the reaction rate constant against reverse temperature give a straight line from which the activation energy obtained equal (17.908 kJ/mol), their results are shown in Figure 13.

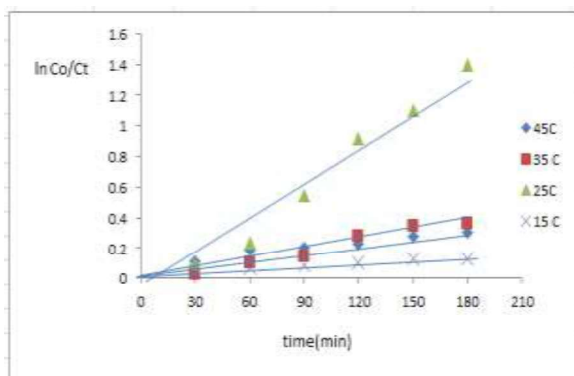


Figure 12: Different temperature of nanoparticle TiO<sub>2</sub>/AQ (0.075g/l), p-N.T (1x10<sup>-4</sup>M), pH5.7

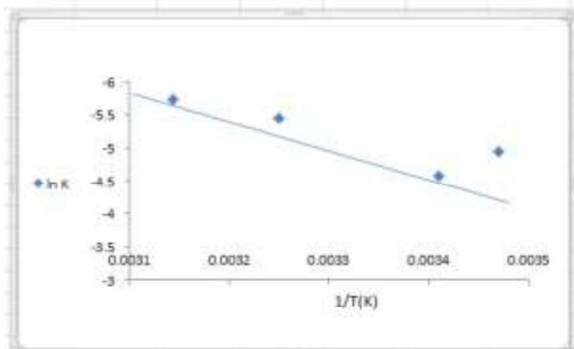


Figure 13: Arrhenius plot for the degradation of p-N.T (1x10<sup>-4</sup>M) irradiated nanoparticle TiO<sub>2</sub>/AQ (0.075g/l)

### Effect of Different Light Sources

The photodegradation of p-N.T were load out under the irradiation of light of three various sources UV lamp (150 watt), visible light (300 watt) and sun light, photocatalytic reaction rate rely largely on the radiation absorption of the photocatalyst.

The photo degeneration activity of p-N.T were found to be extreme at optimal reaction provision pH 5.7, 1x10<sup>-4</sup> M of p-N.T and 0.075 g/l amount of TiO<sub>2</sub>/AQ, down that term in matter, to ensure the diminution in concentration of p-N.T by the photocatalyst. It was spotted that photolysis occupy space by UV-light were lead to be 96%. The 96% photo degeneration was completed under another light source during 180mins; their results are show in Figure 14.

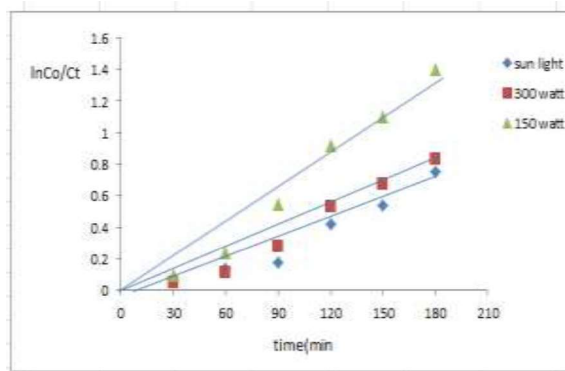


Figure 14: Different light sources for p-N.T (1x10<sup>-4</sup>M), nanoparticle TiO<sub>2</sub>/AQ and pH5.7

### Conclusion

TiO<sub>2</sub>/AQ nanoparticles synthesized through sol-gel method, the addition of AQ in the method of nanoparticle production cause important changes in texture. X-ray diffraction measurement revealed that the particle size was (24.19nm) of TiO<sub>2</sub>/AQ. The SEM and TEM were showed the formation of spherical shaped nanoparticle. A considerable reduction in pore volume and surface area are proportional to that of the pure titanium dioxide. It is apparent that the band gap shifts towards lower values in presents AQ is found (3.05 eV) that indicates numbers of free electrons is available for charge conduction. The TiO<sub>2</sub> /AQ prepare by sol-gel technique exhibit relatively high photocatalytic efficiency in the photo degeneration of p-NT. The photo degeneration of p-nitrotoluene when 0.075 gm.l<sup>-1</sup> of TiO<sub>2</sub>/AQ nanoparticle at pH 5.7 by 150 watt that photocatalyst degenerate p-NT up to 96%.

### References

- [1] R. X. Hailin.L, "photocatalytic activity of Mo+ Fe Co-doped Titanium Dioxide Nanoparticles prepared by Sol-Gel method, " *Vol 28, No.1*, p. 44, 2012.
- [2] C. W.-N. C. C.-F. Hua.D, "Low temperature preparation of Nano TiO<sub>2</sub> and its application as antibacterial agents, " *Trans Nonferrous Met.Soc.China 17*, pp. 700-703, 2007.
- [3] I.-H. Amin.N.M, "synthesis and characterization of Nano-structure TiO<sub>2</sub> thin film prepared by sol-gel spin coating

- method, " *Journal of Applied Sciences Research*. Vol.9, No.3, pp. 1960-1965, 2013.
- [4] K. F. Byranand.M.M, " Review on synthesis of Nano-TiO<sub>2</sub> via Different Methods, " *J.of Nanostructures* 3, pp. 1-9, 2013.
- [5] A. Sayilkan.F, "Characterization of TiO<sub>2</sub> Synthesized in Alcohol by a sol-gel process: the effects of annealing temperature and acid catalyst, " *Turk.J.Chem* 29, pp. 697-706, 2005.
- [6] C. Qi.L, "Synthesis and characterization of CdS nanoparticles stabilized by double - Hydrophilicblock copolymers, " *Nano letters*, Vol 1, No.2, pp. 61-65, 2001.
- [7] A. A. Thangavelu.K, "Preparation and characterization of Nanosized TiO<sub>2</sub> powder by sol-gel precipitation Route, " *International Journal of Emerging Technology and Advanced Engineering*, Vol 3, No.1, 2013.
- [8] R. Vijaylakshmi.R, "Synthesis and characterization of Nano-TiO<sub>2</sub> Via different methods, " *Scholars Research Library Archives of applied Science Research*. Vol 4, No.2, pp. 1183-1190, 2012.
- [9] P. J. Stefanska.K.S, "The influence of addition of a catalyst and chelating agent on the properties of titanium dioxide synthesized Via the sol-gel method, " *J. Sol-Gel Sci. Technol*, 75, pp. 264-278, 2015.
- [10] L. S. B. O. Starowicz.Z, "Photochemical silver nanoparticales deposition on sol-gel TiO<sub>2</sub> for plasmonic properties utilization, " *J.Sol-Gel.Sci Technol*.73, pp. 563-571, 2015.
- [11] V. S. R. Balachandran.K, "Synthesis of nano TiO<sub>2</sub>-SiO<sub>2</sub> composite using Sol-Gel method: effect on size, surface morphology and thermal stability, " *International Journal of Engineering Science and Technology*, Vol 2, No.8, pp. 3695-3700, 2010.
- [12] N. Tumuluir.A, "Band gap determination using Taucs plot for LiNbO<sub>3</sub> thin films, " *International Journal of Chem. Tech. Research*. Vol.6, No.6, pp. 3353-3356, 2014.
- [13] N. Komarneni S., "Solvothormal Hydro-thermal synthesis of metal oxides and metal powders with and without microwaves, " *Verlag der Zeitschrift fur naturfoe schung, Tubingen*, 65, pp. 1033-1037, 2010.
- [14] L. C. D. Trinh.D.T.T, "Investigation of intermediate compounds of phenol in photocatalysis process, " *International Journal of chemical engineering and applications*, Vol 7, No.4, 2016.
- [15] m. H. L. Friesen.D.A, "Factors influencing relative efficiency in photo-oxidations of organic molecules by Cs<sub>3</sub>PWO and TiO<sub>2</sub> colloidal photocatalysts, " *Journal of photochemistry and photobiology A*, Vol.133, No.3, pp. 213-220, 2000.